METAL IN UREILITES: SIDEROPHILE ELEMENTS FROM LA-ICP-MS.

[1]R.D. Ash, [2]C.A. Goodrich, [1]W.F. McDonough and [3]J.A. Van Orman. [1]Dept. of Geology, Univ. of Maryland, College Park, MD 20742 USA. rdash@geol.umd.edu. [2]Dept. of Physical Sciences, Kingsborough Community College, Brooklyn, NY 11235 USA. cgoodrich@kingsborough.edu. [3]Dept. of Geological Sciences, Case Western Reserve, Cleveland, OH 44120 USA

Introduction: Bulk ureilites have near chondritic abundances of siderophile elements [1-7], showing no correlation with Fe contents (~5-16 wt.%) or *mg* (molar Mg/[Mg+Fe]). These observations are difficult to reconcile with any igneous model for their silicates [8]. We address this problem through detailed characterization of the metal phases in ureilites [9], and petrologic modelling [10]. Here we present siderophile element data from LA-ICP-MS for metal, oxidized metal and silicates in initial samples.

Samples and Analytical: Samples were olivine-pigeonite ureilites Kenna (Fo 79), ALHA77257 (Fo 86) and EET 90019 (Fo 89), as well as augite-bearing ureilites META78008 (Fo 76), Hughes 009 (Fo 87) and ALH 82130 (Fo 95). Petrographic descriptions and compositions from EMPA are given in [9]. LA-ICP-MS analyses were perfomed at the Univ. of Md. using a ThermoFinnigan Element 2 single collector magnetic sector ICP coupled to a New Wave UP213 laser. Laser power was between 2-3mJcm^{-2}, with a repetition rate of 5-7Hz. Spotsizes were determined largely by mineral grain size and ranged from 15µm-80µm. Ablated material was entrained in a stream of He to transport to the mass spectrometer. Coahuila, NIST610 and Babb's Mill (Troost) were used as standards, normalizing to Ni or Fe [9]. Analyzed elements were Si, Cr, Mn, Fe, Co, Ni, Cu, Zn, Ga, Ge, As, Mo, Ru, Rh, Pd, Sb, W, Re, Os, Ir, Pt and Au. A subset of these are presented for comparison to bulk rock data (plots CI-normalized).

Results: Unsurprisingly, in all cases silicate cores show lower siderophile abundances (orders of magnitude) than grain boundary and included metal.

Kenna (Fig. 1a): Metal in our section of Kenna is almost all oxidized, resulting in large apparent variations in abundances of siderophile elements. Nevertheless, the average of these analyses provides a reasonable fit to the bulk rock at the 8% level. We observed one preserved metal grain in graphite. Both the metal and the graphite itself (due to tiny metal inclusions?) show a siderophile element pattern similar to that of the bulk rock. One olivine reduction rim has higher abundances than cores. Au data (not shown) are erratic; we suspect the section was once Au-coated.

ALHA77257,104 (Fig. 1b): Most of the metal in this sample is preserved. Analyses of grain boundary metal show a consistent pattern very similar to that of the bulk rock, and 1.7% metal could account for the bulk siderophile abundances. Cohenite-metal-phosphide-sulfide spherules in pigeonite show siderophile abundances essentially identical to those of the grain boundary metal. One spherule in olivine has a more fractionated pattern. One olivine reduction rim has higher abundances than cores.

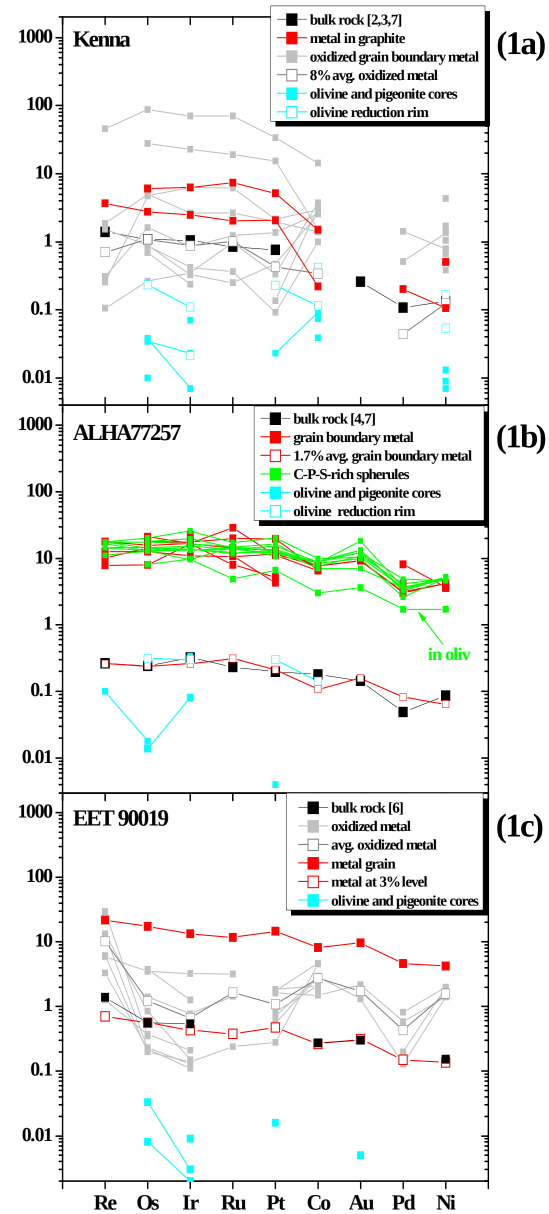

EET 90019,13 (Fig. 1c): All grain boundary metal in this section was oxidized. We found one bleb of unaltered metal in a vein in olivine. Siderophile element abundances of the oxidized metal are variable and the average is not a good match to the bulk rock patttern. The metal has a pattern nearly identical to that of the bulk rock and could account for it at 3%.

META78008,49 (Fig. 2a): Most of the grain boundary metal in this sample is preserved and shows a pattern similar to that of the bulk rock. Analyses of metal in graphite show a pattern nearly identical to that of the bulk rock. Their average provides a good fit to the bulk rock at the 3.5% level. One larger bleb of metal in a reduction rim has abundances similar to those of grain boundary metal.

ALH 82130,9 (Fig. 2b): Most of the grain boundary metal in this section is oxidized. Siderophile element patterns of oxidized metal, and a few preserved metal grains, are mostly similar to the bulk rock pattern and (except for Re and possibly Au) their average could account for the bulk rock at the 5% level.

Hughes 009, B1 (Fig. 2c): Most grain boundary metal in this sample is oxidized and brecciated [9,11]. However, one preserved area consists of a eutectic-like intergrowth of schreibersite and metal. Analyses of the two phases recombined in modal proportions give a pattern for this intergrowth which differs from that of the bulk rock in having higher abundances of Co, Pd and Ni relative to PGE. Analyses of oxidized metal show a similar tendency. Au data (not shown) are erratically high due to previous Au-coating.

Interpretations: These data show that grain boundary metal (or its oxidized equivalent) is the main host of siderophile elements in ureilites. In each sample it shows siderophile element patterns that are similar to that of the bulk rock and abundances consistent with observed modal abundances. Nevertheless, in many samples terrestrial oxidation has disturbed Re [12] and Co relative to PGE, and produced scatter in siderophile abundances (this may also be due to effects of porosity on the analyses). Effects of late reduction [9] are not pronounced in trace elements. Silicate cores do not contain significant siderophiles compared to metal. However, some reduction rim metal shows higher abundances, indicating that it did not remain isolated despite rapid cooling [8,11].

The cohenite-metal-phosphide-sulfide spherules have textures and C,P,S-rich compositions suggesting that they were liquids and could have been complementary to residual grain boundary metal [9,13]. However, data obtained here show that spherules and grain boundary metal have nearly identical trace siderophile element abundances. We address this contradiction in [10].

Grain boundary metal in Hughes 009 appears to be an Fe-P eutectic melt [9]. Trace element data (e.g. high Co, Pd Ni) also suggest melt characteristics, although this may be due to shock remobilization [11].

References: [1] Wänke H. et al. (1972) *Meteorit.* **7**, 579. [2] Boynton W.V. et al. (1976) *GCA* **40**, 1439. [3] Janssens M-J. et al. (1987) *GCA* **51**, 2275. [4] Warren P.H. and Kallemeyn G.W. (1992) *Icarus* **100**, 110. [5] Warren P.H. and Kallemeyn G.W. (1994) *LPS* **25**, 1465. [6] Warren P.H. et al. (2006) *GCA* **70**, 2104. [7] Rankenburg K. et al. (2008) *GCA* **72**, 4642. [8] Mittlefehldt D.W. et al. (1998) In Planetary Materials. *Rev. Mineral.* **36**. [9] Goodrich C.A. et al., this volume. [10] Van Orman J.A. et al., this volume. [11] Goodrich C.A. et al. (2001) *GCA* **65**, 621. [12] Rankenburg K. et al. (2007) *GCA* **71**, 2402. [13] Goodrich C.A. and Berkley J.L. (1986) *GCA* **51**, 2255.

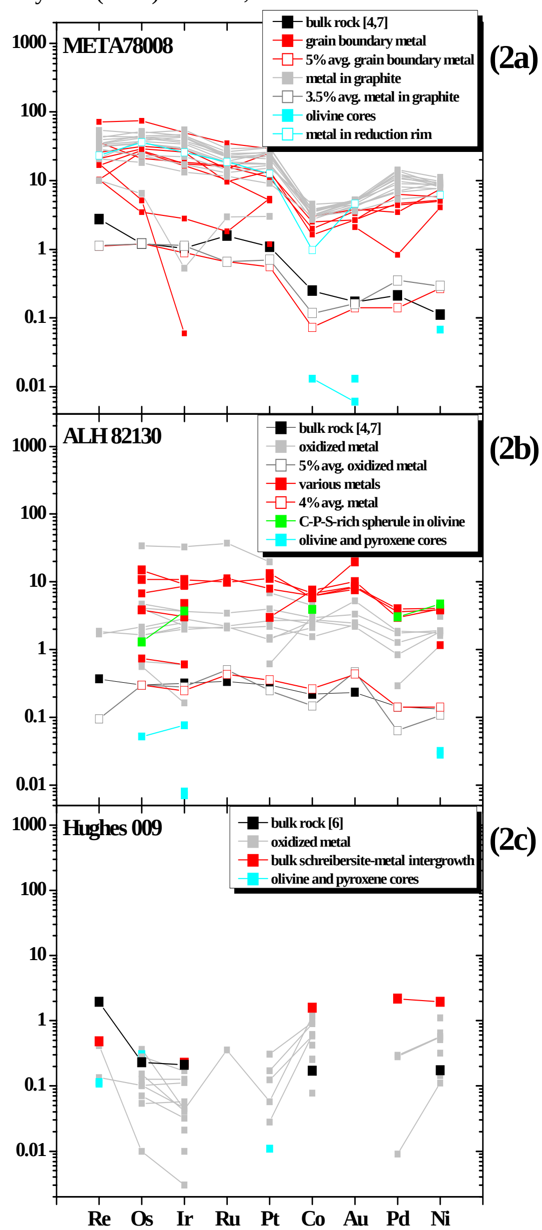

We gratefully acknowledge NASA grants NNX08AH76G (WFM/RDA) and NNX08AG63G (CAG).